Dynamic Mechanical Properties of Polyimide/ Poly(silsesquioxane)-Like Hybrid Films

MEI-HUI TSAI, WHA-TZONG WHANG

Department of Materials Science and Engineering, National Chiao Tung University, Hsin Chu 300, Taiwan, People's Republic of China

Received 19 May 2000; accepted 20 November 2000

ABSTRACT: Polyimide/poly(silsesquioxane)-like (PI/PSSQ-like) films have three-dimensional structure with linear PI blocks and a crosslinked PSSQ-like structure. They have higher thermal stability and char yields than pure PI from 4,4′-diaminodiphenyl ether and 3, 3′-oxydiphthalic anhydride (ODPA). In a series of *X*-PIS [PI modified with *p*-aminophenyltrimethoxysilane (APTS), where *X* is the molecular weight of each PI block] hybrid films, decreasing the PI block chain length enhances the storage modulus, tensile modulus, and glass-transition temperature (T_g) but reduces the α-relaxation damping peak intensity, density, and elongation. The change in the former three properties may be caused by an increase in the crosslinking density and rigidity of the network structure. The changes in the next two properties are caused by an increase in the free volume or the PI interblock separation and decreases in the interblock PI chain interaction. The change in the last property (i.e., a decrease in elongation) is related to the increase in the rigidity of the network structure. The activation energy of the α transition depends on the chain length of the PI block. A maximum value is reached at the chain length of 10,000 because of two different factors: crosslinking density and free volume. In a series of *X*-PIS-*y*-PTS [*X*-PIS modified with phenyltrimethoxysilane (PTS), where *y* is the weight-ratio percentage of PTS to APTS–polyamic acid] films with a constant PI block length, the storage modulus, tensile modulus, T_g, density, and α-relaxation damping peak intensity decrease with the PTS content. This could be because of the increase of the PSSQ-like domain size with the PTS content, which leads to the introduction of more free volume or interblock separation and to a decrease in the interblock chain interaction force. © 2001 John Wiley & Sons, Inc. J Appl Polym Sci 81: 2500–2516, 2001

Key words: PI/PSSQ-like; crosslinking density; dynamic mechanical analysis; activation energy; free volume

INTRODUCTION

Poly(silsesquioxane) (PSSQ) has been widely used as a dielectric material in the manufacture of integrated circuits,[1–3] especially for ultra-large-scale circuits, because of its low dielectric constant and reasonable film formation. The film, forming through the hydrolysis and condensation of its precursor, exhibits excellent interfacial adhesion with the inorganic substrate and even endures hostile environments in chemical–mechanical polishing processes.[2,3] However, it is brittle. Aromatic polyimides (PIs) are also popularly used in the electronic and microelectronic industries[4–6] because of their excellent thermal stability, tough mechanical properties, and low dielectric constants. However, pure aromatic PIs possess limitations for reliable performance ap-

Correspondence to: W.-T. Whang (wtwhang@cc.nctu.edu.tw).

Journal of Applied Polymer Science, Vol. 81, 2500–2516 (2001)

plications. For example, they have poor interfacial adhesion with inorganic substrates if they are not modified with silicon-related agents or inorganic agents.[7–11] Therefore, the hybridization of aromatic PIs and PSSQ may result in a new type of material that possesses the balanced properties of both virgin materials and keeps their low dielectric characteristics.[12–14]

PSSQ may be prepared from monoalkyltrialkoxysilanes[15] or monoaryltrialkoxysilanes[16] and tetraalkoxysilanes[17,18] through hydrolysis and condensation in a sol–gel process. The PI/PSSQ-like hybrid composites (nanocomposites) are prepared from a PI precursor containing phenyltrialkoxysilane at two chain ends or monoaryltrialkoxysilane in a sol–gel process. The performance reliability[19] of the material is very important in electronic applications because it is dependent on chemical composition and physical structure.

Dynamic mechanical analysis (DMA) is a sensitive analysis technique[20–23] that can measure the properties of materials as they are deformed under periodic stress. It is particularly useful for the evaluation of the viscoelastic characteristics of polymers. Usually, the dynamic mechanical characteristics of polymeric materials are time-, frequency-, and temperature-dependent and may correlate with the details of chemical composition and physical structure. Because PI/PSSQ-like hybrid composite films are new materials, there is a lack of systematic studies of their dynamic mechanical characteristics to correlate with their chemical compositions and physical structures. The low dielectric PI/PSSQ-like nanocomposite material[12] and long-term performance reliability for PI/PSSQ-like hybrid films[19] have been discussed in other articles. In this study, we investigated the dynamic mechanical characteristics of PI/PSSQ-like hybrid composites, including frequency-dependent relaxation, relaxation activation energy, storage modulus, loss modulus, damping, and static mechanical properties. We also tried to correlate the properties with the silica component, the PSSQ-like content, the PI block chain length, and the crosslinking density. The densities were measured to determine the possible free volume in the films, and they were correlated to the dynamic mechanical properties.

EXPERIMENTAL

Materials and Their Purification

3,3′-Oxydiphthalic anhydride (ODPA; 98%) from Tokyo Chemical Industry (Japan) was purified by recrystallization from acetic anhydride and then dried in a vacuum oven at 125°C overnight. 4,4′-Diaminodiphenyl ether (ODA; 98%) from Loncaster was subjected to a thermal treatment in a vacuum oven at 120°C for 3 h prior to use. *N*-Methyl-2-pyrrolidone (NMP) from Tedia Co. (USA) was dried over molecular sieves. *p*-Aminophenyltrimethoxysilane (APTS; 95% para and 5% meta) from Gelest Inc. and phenyltrimethoxysilane (PTS; 98%) from Lancaster were used as supplied.

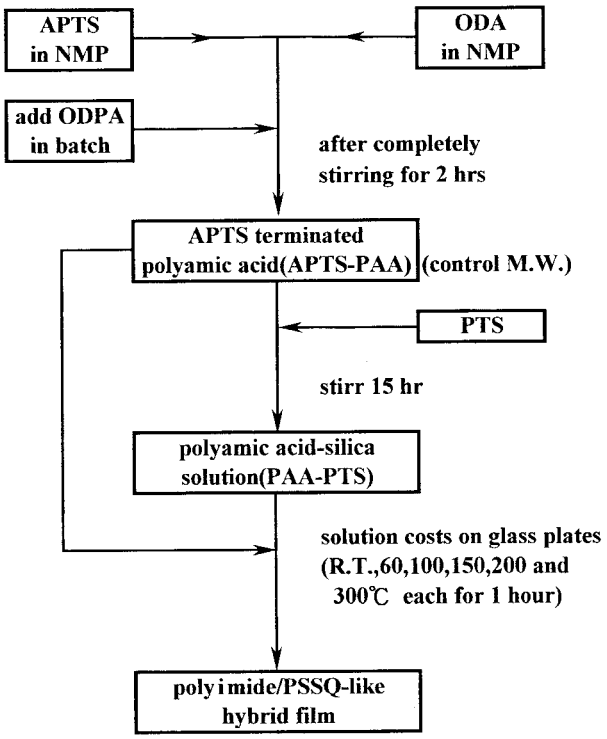

Scheme 1

Synthesis of Aminophenyltrimethoxysilyl-Terminated Polyamic Acid (APTS–PAA) Oligomers[12–14,19,24]

The reaction is shown in Scheme 1. A three-necked flask (250 mL) was first purged with nitrogen gas to remove the moisture prior to the addition of the reagent. The polycondensation was carried out in the flask via the addition of the diamine ODA, the monoamine APTS, and a dianhydride in NMP under a nitrogen stream at room temperature. APTS was used to control the chain length of trimethoxysilyl-terminated PAA. In a typical reaction to prepare the APTS-terminated PAA with a molecular weight of 5000, 0.04676 mol of ODPA was added to a solution containing 0.04176 mol of ODA and 0.01 mol of APTS in 75 g

of NMP. ODPA was introduced into the solution in five portions. This was done to ensure the complete dissolution of the previous portion before the addition of a fresh portion. After the dissolution of all ODPA, the reaction mixture was further stirred for 2 h at room temperature. The PAA solution had a 25% (w/w) solid content.

Preparation of PAA–PTS Solution

The APTS–PAA solution mentioned previously was divided into five equal portions (20 g of solution for each), and each was added to different weights of PTS: 0.4, 0.8, 1.2, 1.8, 2.5, 3.5, 5.0, and 7.0 g [PTS/APTS–PAA (w/w) = 8, 16, 24, 36, 50, 70, 100, and 140, respectively]. Stirring was continued at room temperature for 15 h, yielding a yellow PAA–PTS homogenous viscous solution.

Preparation of PI/PSSQ (PI/PSSQ)-Like Hybrid Films

APTS–PAA and PAA–PTS solutions were cast onto glass plates with a thickness of 250 μm and then kept at room temperature in air (relative humidity $\geq$ 70 %) at least 40 min to absorb water for a sol–gel process in the trialkoxysilane units. The cast films were subjected to step-heating at 60, 100, 150, 200, and 300°C, each for 1 h. The thickness of PI/PSSQ-like films from APTS–PAA and PAA–PTS ranged from 30 to 50 μm. The reaction of APTS–PAA and PAA–PTS into PI/PSSQ-like hybrids (*X*-PIS, where *X* is the molecular weight of each PI block, and *X*-PIS-*y*-PTS, where *y* is the weight-ratio percentage of PTS to APTS–PAA) through hydrolysis and condensation is described in Scheme 1. The structures of PSSQ and the PI/PSSQ-like hybrid film are shown in Scheme 2. The PI/PSSQ-like hybrid films from APTS–PAA and PAA–PTS film were encoded as *X*-PIS and *X*-PIS-*y*-PTS, respectively.

Characterization

The dissolution tests of the pure PI and *X*-PIS and *X*-PIS-*y*-PTS hybrid films were measured in an organic solvent at 80°C. Infrared spectra were obtained with a Nicolet PROTEGE-460 Fourier transform infrared spectrophotometer. The density of the prepared films was determined with an electronic densometer SD-120L with four pieces of the film, 3 $\times$ 3 cm each. The density data reported here are the averages of the four testing values. Thermogravimetric analysis (TGA) was carried out with a DuPont Instruments 951 machine at a heating rate of 10°C/min from 80 to 800°C under nitrogen. The tested sample weighed about 10 mg. The TGA test was performed once. Dynamic mechanical properties were measured with a TA Instruments DMA 2980 dynamic mechanical analyzer at a heating rate of 3°C/min from 60 to 350°C. The samples (20 $\times$ 5 mm) were run at a frequency of 1 Hz with a tension clamp. Multifrequency (0.1, 0.5, 1, 5, and 10 Hz) scans were run at a heating rate of 2°C/min from 240 to 330°C. The DMA data were double-checked. The tensile stress–strain properties were also measured on the same equipment with the controlled force mode. The samples (20 $\times$ 3mm) were elongated at a ramp rate of 4 Newtons/min at room temperature. The tensile stress–strain properties were obtained from an average of five different determinations.

RESULTS AND DISCUSSION

The dissolution tests in Table I show that the pure ODA–ODPA PI was soluble, but the *X*-PIS and *X*-PIS-*y*-PTS films were not soluble. This could be explained by the formation of PSSQ-like three-dimensional silica through the hydrolysis and condensation of trimethoxysilane from APTS–PAA and PAA–PTS[12–14,19] Usually, a trifunctional monomer would easily lead to a crosslinked structure after polymerization, even though the reaction is not complete. That means even though some active functional groups are behind, the crosslinking can still occur in the polymerization of three functional monomers. APTS–PAA and PAA–PTS were thermally converted into the three-dimensional structure of a PI/PSSQ-like hybrid with linear PI blocks and a crosslinked PSSQ-like structure. The terminal or added PTS became phenyltrihydroxylsilane after hydrolysis with the water in air or from the imidization of PAA. Then, it was converted into a PSSQ-like structure after condensation. PSSQ-like means that it may have formed a structure like PSSQ but may not have been so perfect as PSSQ because each methoxy group of PSSQ-like hybrids did not sol–gel completely like PSSQ.

The infrared spectra of pure ODA–ODPA PI, 5000-PIS, and 5000-PIS-24-PTS are shown in Figure 1. The asymmetric carbonyl stretch at 1778 cm^{-1} and the C—N stretch at 1380cm^{-1}, which are characteristic of PI, are apparent in Figure 1. The very weak broad band in the range 3700–3200 cm^{-1} was attributed to OH stretching. Pure PI had no significant infrared absorp-

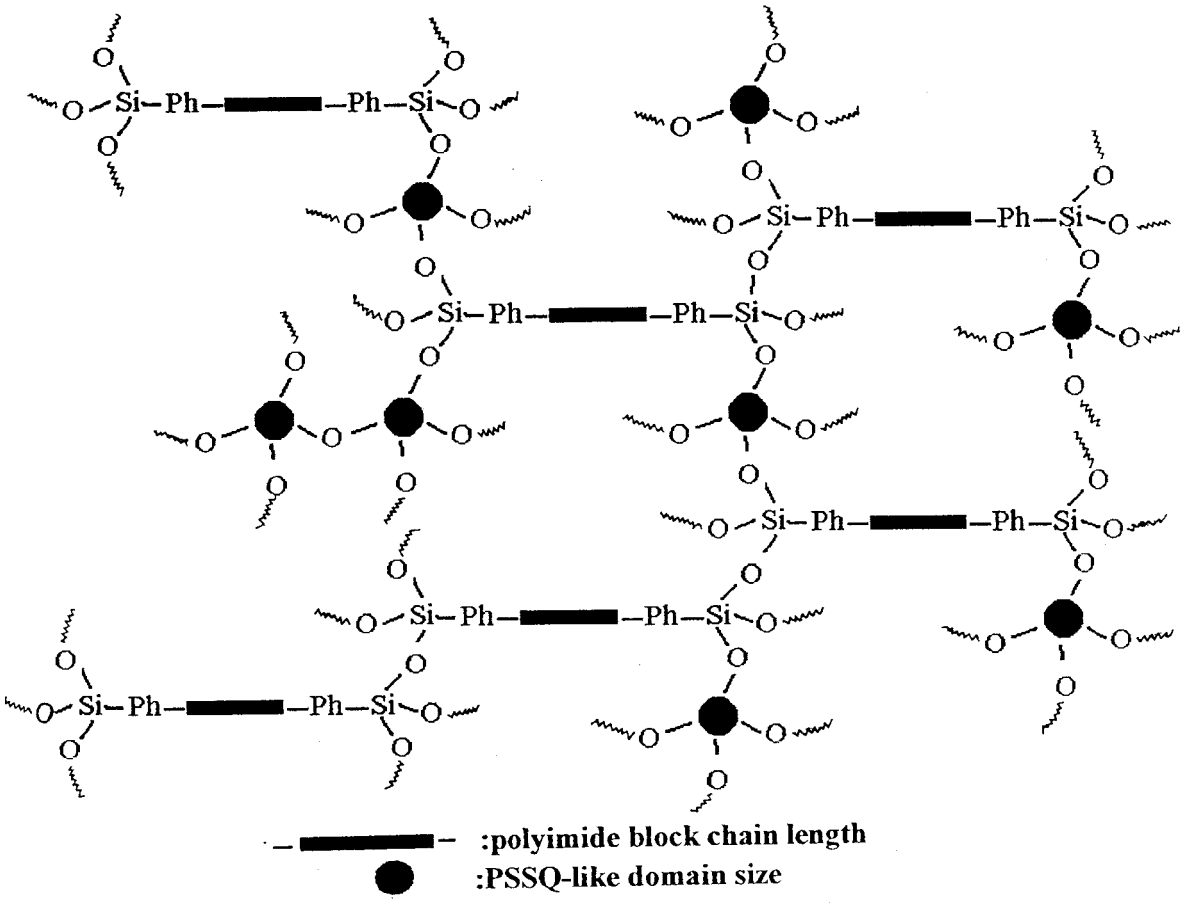

Ideal PI/PSSQ

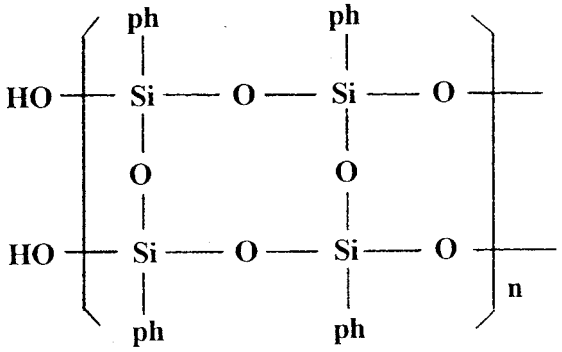

PSSQ

Scheme 2

Table I Dissolution Tests of Pure ODA–ODPA PI, *X*-PIS, and *X*-PIS-*y*-PTS at 80°C

	Solvent[a]				
Sample Code	NMP	DMAc	DMF	DMSO	Pyridine
5000-PIS	−	−	−	−	−
5000-PIS-24-PTS	−	−	−	−	−
5000-PIS-70-PTS	−	−	−	−	−
10,000-PIS	−	−	−	−	−
10,000-PIS-24-PTS	−	−	−	−	−
10,000-PIS-70-PTS	−	−	−	−	−
Pure PI	+	+	±	+	+

Dissolution tests: − = insoluble, + = soluble, and ± = partially soluble.
[a]DMAc = *N,N*-dimethylacetamide; DMF = *N,N*-dimethylforamide; DMSO = *N,N*-dimethylsulfoxide.

tion in this region, whereas 5000-PIS and 5000-PIS-24-PTS hybrid films presented a weak and wide band in this region. This difference may be explained by the steric hindrance by phenyl groups (or methyl side groups[25,26]) on the silicon atom, inhibiting the formation of Si—O—Si bonding in the hybrid films and leaving traces of hydroxyl groups inactive.

The dynamic thermogravimetric curves and the differential thermogravimetric curves of the pure ODA–ODPA PI, 5000-PIS, 5000-PIS-16-PTS, and 5000-PIS-100-PTS films are shown in Figure 2. The pure PI and 5000-PIS-*y*-PTS films exhibited one-step decomposition. The former demonstrated a maximum decomposition rate at a high temperature greater than 580°C and some

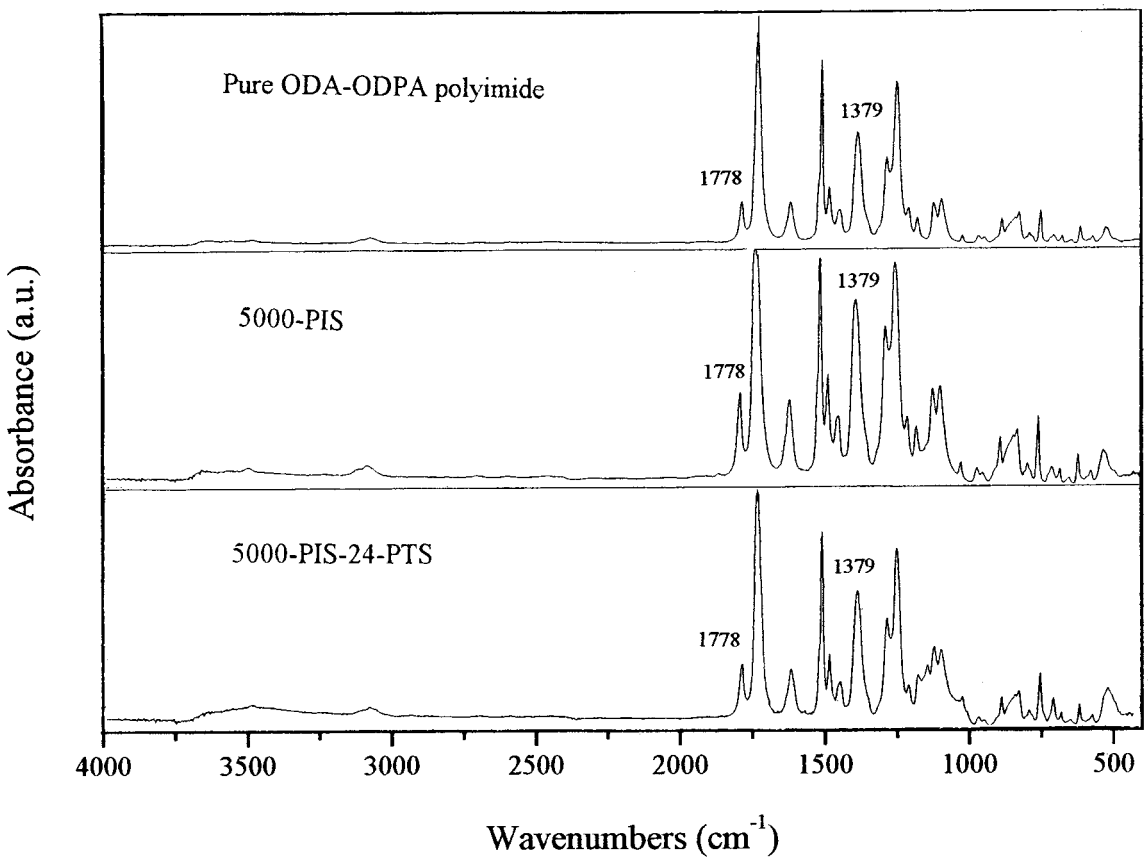

Figure 1 Infrared spectra of pure ODA–ODPA PI, 5000-PIS, and 5000-PIS-24-PTS.

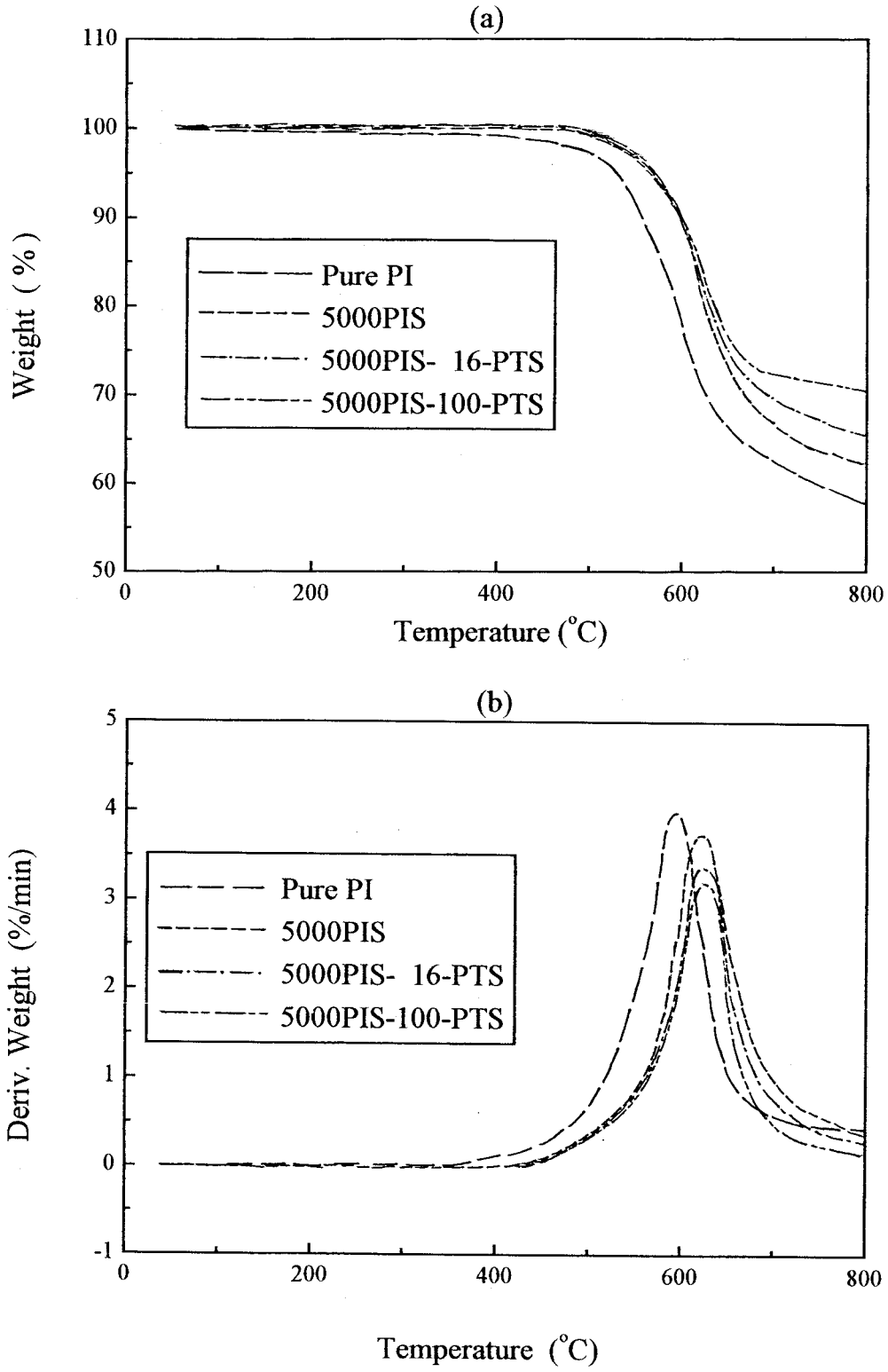

Figure 2 Dynamic thermogravimetric curves and differential thermogravimetric curves of pure ODA–ODPA PI, 5000-PIS, 5000-PIS-16-PTS, and 5000-PIS-100-PTS.

weight loss at temperatures below 400°C. The latter demonstrated a maximum decomposition rate at a high temperature greater than 618°C. There was no weight loss at temperatures below 400°C, although some hydroxyl groups may have been residual in the PSSQ-like structure. That

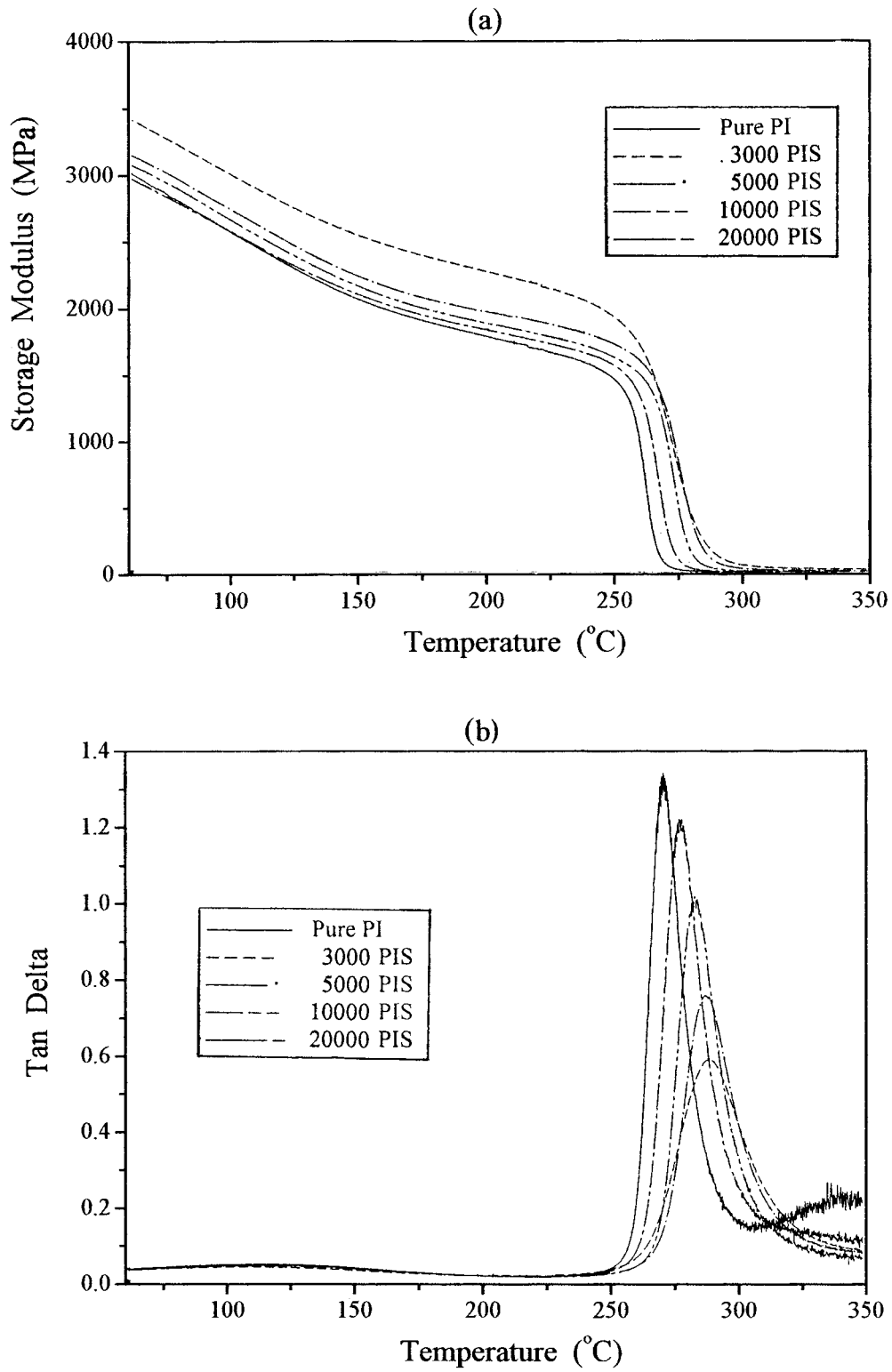

Figure 3 (a) Storage modulus and (b) tan δ of DMA for pure ODA–ODPA PI, 20,000-PIS, 10,000-PIS, 5000-PIS, and 3000-PIS.

means the residual hydroxyl groups encountered steric hindrance, preventing the completion of condensation. However, the *X*-PIS and *X*-PIS-*y*-PTS films were still more thermally stable than pure PI. The former also had a higher char yield than the latter at 800°C.

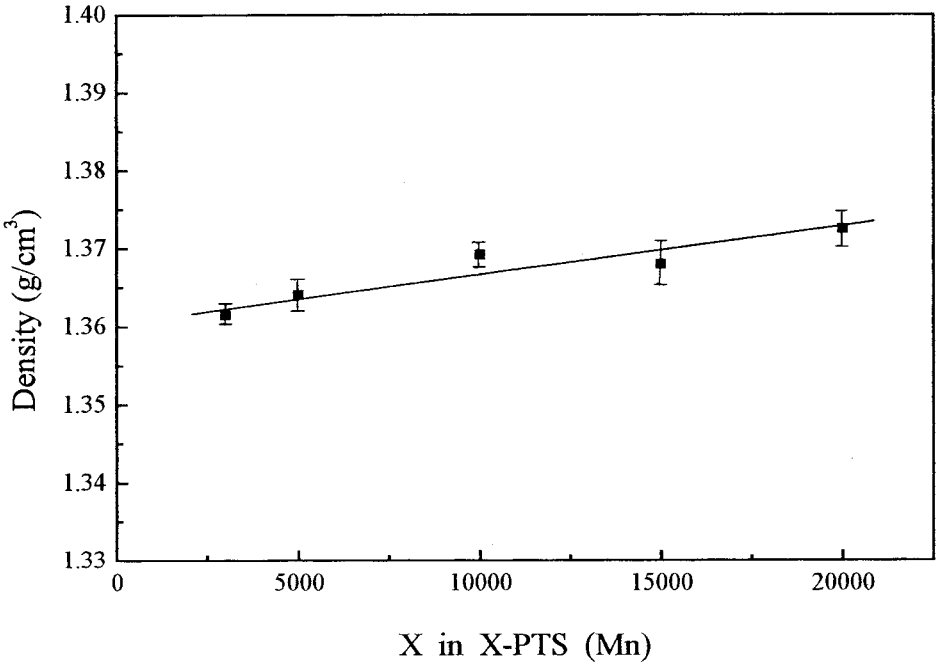

Figure 4 Densities of *X*-PIS.

The storage modulus and tan δ (where tan δ is the loss factor that is equal to loss modulus/storage modulus) curves of DMA for the pure ODA–ODPA PI and *X*-PIS hybrid films are shown in Figure 3.

Figure 3(a) shows the storage modulus of *X*-PIS and pure ODA–ODPA PI. They all were temperature-dependent, decreased gradually at temperatures below 250°C, and finally showed an abrupt drop at 250–290°C. Figure 3(a) also shows that the shorter the PI block chain length was, the higher the storage modulus was, whether at low or high temperatures. The *X*-PIS hybrid films with shorter PI block chain lengths had a higher crosslinking density and higher modulus and were more rigid. Incorporating the PSSQ-like structure into the PI structure promoted the modulus and high-temperature reliability[19] of the PI material. Figure 3(a) also showed that although the pure ODA–ODPA PI almost failed at 265°C, some *X*-PIS films still had a reasonable modulus to retain the structure.

As shown in Figure 3(b), all the PI hybrid films *X*-PIS and the pure PI film exhibited two transition peaks in the tan δ curves, one small peak near 125°C and another strong peak in the range of 260–300°C. The small peak was less sensitive to the composition, but the latter strongly depended on the PI block chain length. To understand the origin of the small peak, the sample films were first isothermally heated at 205°C for 30 min in the DMA instrument to get rid of the absorbed water or residual solvent before the actual DMA measurements. After the isothermal heating, the samples were cooled down to 60°C before the DMA tests were started at 4°C/min. Because the peak near 125°C was independent of the PI block chain length, the small peak was most probably caused by the local motion of PI,[27–30] irrelevant to water, solvent, or the PSSQ-like structure. It was a kind of β-transition peak. However, the strong peak in the range of 250–300°C depended strongly on the PI block chain length. This transition temperature, the second peak, decreased, and the peak intensity increased with the chain length. This strong peak may have been caused by the main-chain relaxation of the PI block, a glass-transition relaxation.[27–30] In the PI/PSSQ-like hybrid films, the crosslinking density decreased with the PI block chain length. Usually, crosslinking in polymers limits chain movement. Higher crosslinking density leads to a higher hindrance from chain movement so that the movement occurs only at higher temperatures. Therefore, the longer the PI block chain length is, the lower the T_g is. Pure ODA–ODPA PI exhibited the lowest T_g but the highest damping peak intensity. The damping may have resulted from polymer chain friction during chain movement. The chain friction is caused by intermolecular chain interaction. The

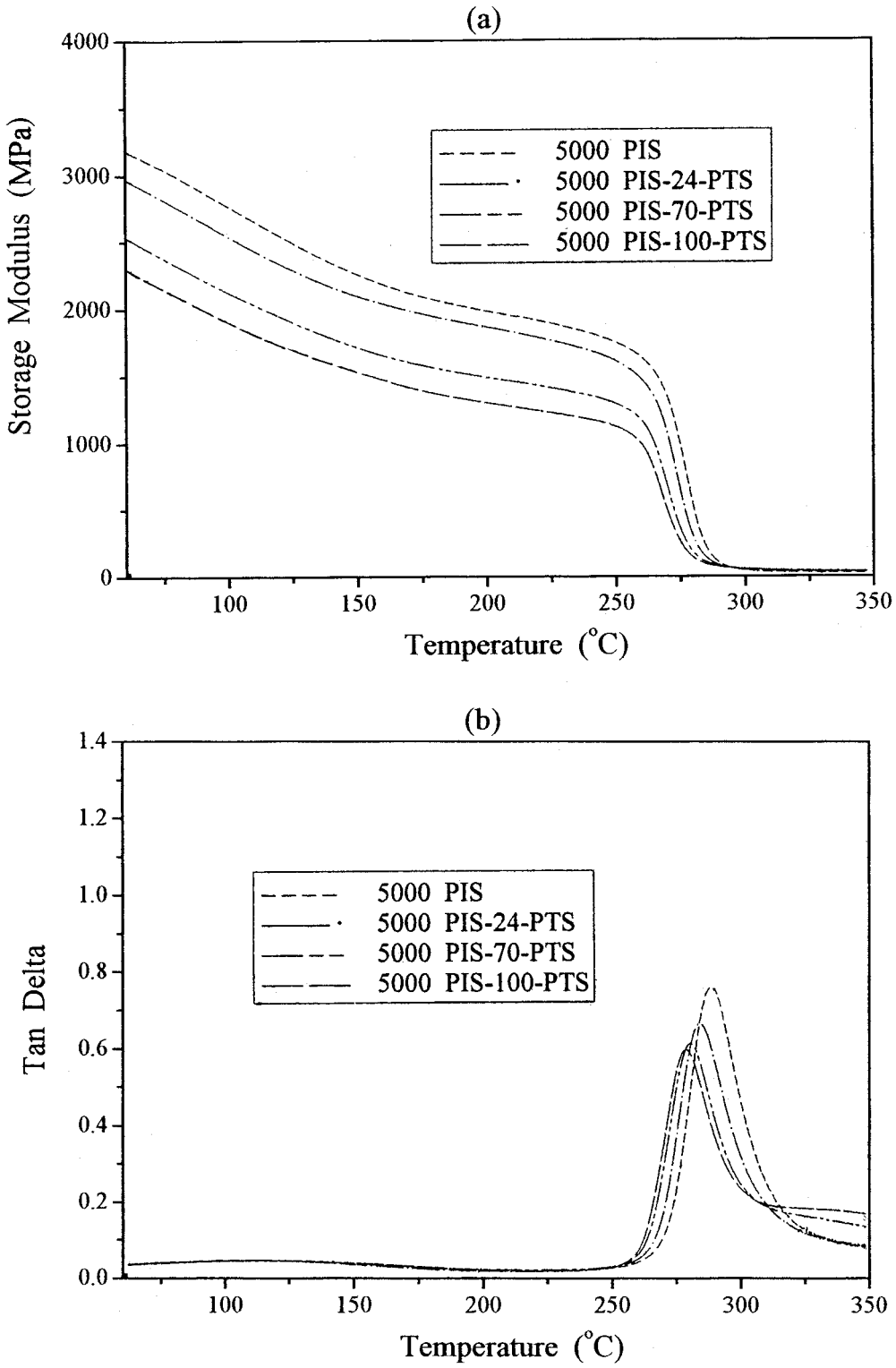

Figure 5 (a) Storage modulus and (b) tan δ of DMA for 5000-PIS, 5000-PIS-24-PTS, 5000-PIS-70-PTS, and 5000-PIS-100-PTS.

chain friction in the movement dissipates heat; this is an irreversible energy consumption. Therefore, low damping in the tan δ curve indicates a lower interaction force between molecular chains, and a high damping indicates high chain interaction force. The damping peak in-

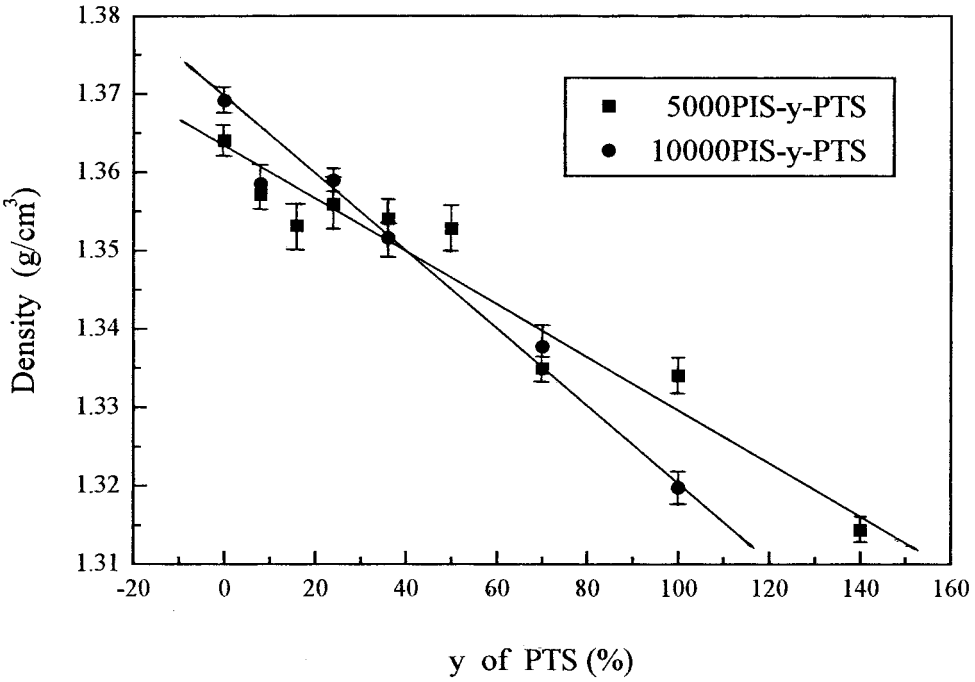

Figure 6 Densities of 5000-PIS-*y*-PTS and 1000-PIS-*y*-PTS hybrid films.

tensity clearly showed that the longer the PI block chain length was, the higher the chain interaction force was.

Figure 4 shows the dependence of the densities of *X*-PIS hybrid films on the PI block chain length. It indicates that the density of the film increased with the PI block chain length. This means that the free volume in the films decreased with the PI block chain length. The molecular chains of aromatic PI are semirigid. In the network structure, the PI/PSSQ-like hybrid film with shorter PI blocks behaved less flexibly, and the interblock

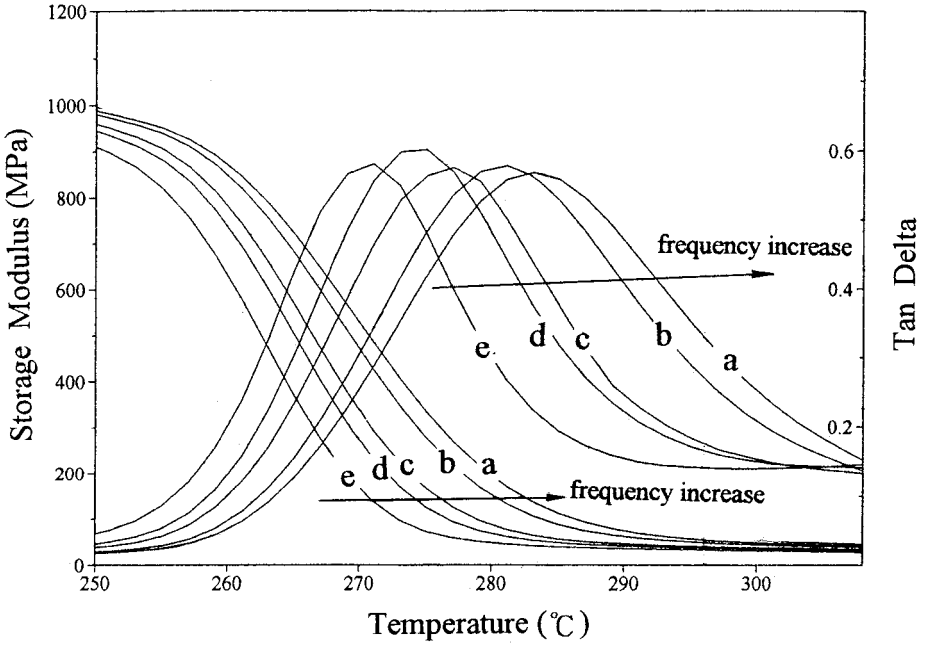

Figure 7 Frequency dependence of the storage modulus and tan δ in DMA for 10,000-PIS-100-PTS: (a) 10, (b) 5, (c) 1, (d) 0.5, and (e) 0.1 Hz.

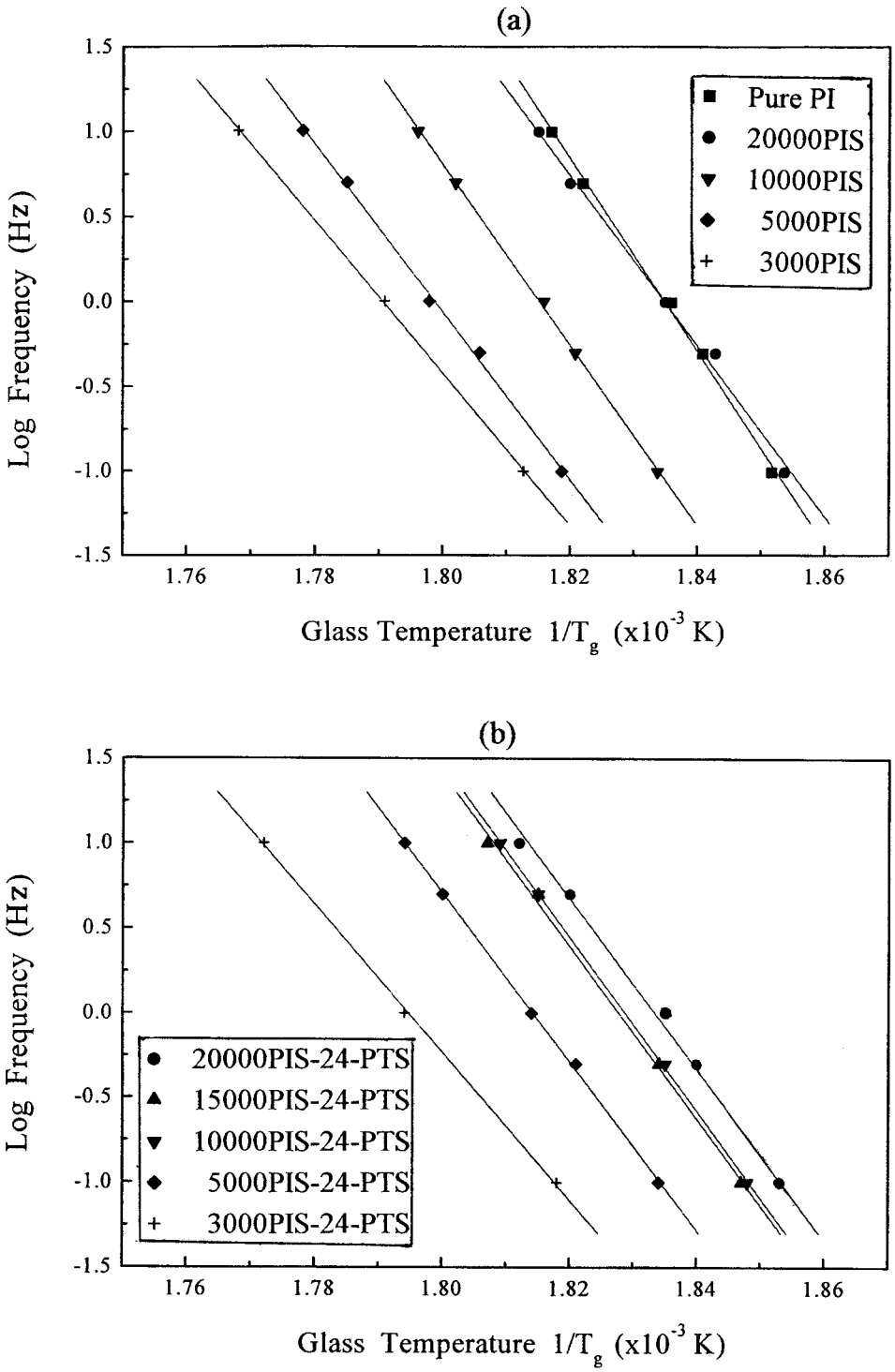

Figure 8 Relationships between the logarithmic frequency and reciprocal peak temperature of tan δ of (a) pure ODA–ODPA PI and *X*-PIS and (b) *X*-PIS-24-PTS hybrid films.

chain distance was slightly enhanced and had a decreasing density. In the other to, this could have been caused by higher flexibility with the longer PI block in the network structure decreasing the interblock chain separation and increasing the density. Moreover, the enhanced interblock chain distance led to lower chain interaction and a lower damping peak.

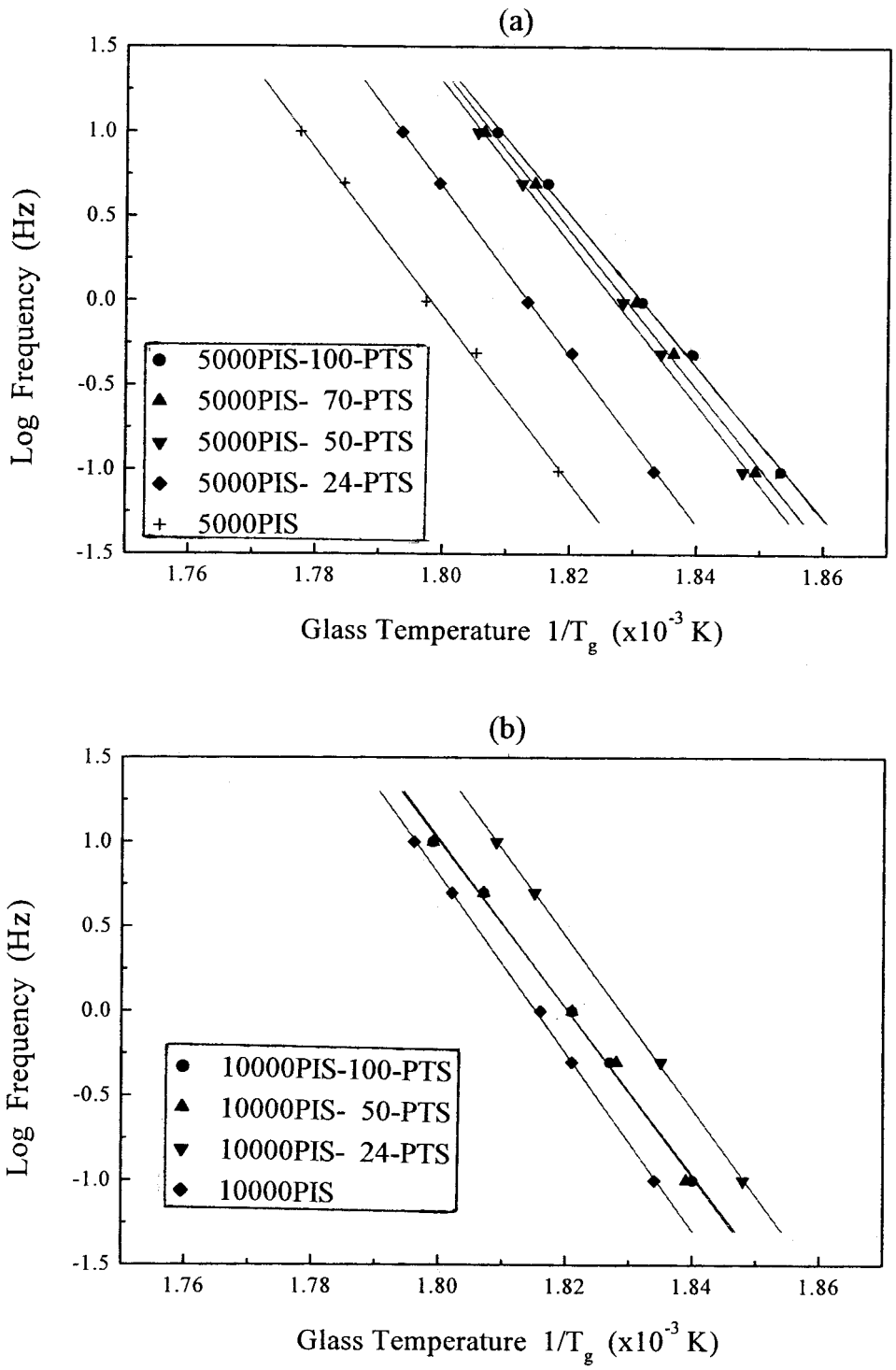

Figure 9 Relationships between logarithmic frequency and reciprocal peak temperature of tan δ of (a) 5000-PIS-*y*-PTS and (b) 10,000-PIS-*y*-PTS.

Figure 5 shows the effect of PTS on the dynamic mechanical properties of 5000-PIS-*y*-PTS. The data shows that higher *y* values led to the decrease in the storage modulus and T_g. The more PTS was in the hybrid films, the lower the storage modulus and T_g were. 10,000-PIS-*y*-PTS hybrid films also showed a similar trend. In the tan δ curves, the damping peak gradually decreased with more PTS. A higher PTS content could form bigger PSSQ-like domain sizes.[12,15] Figure 6

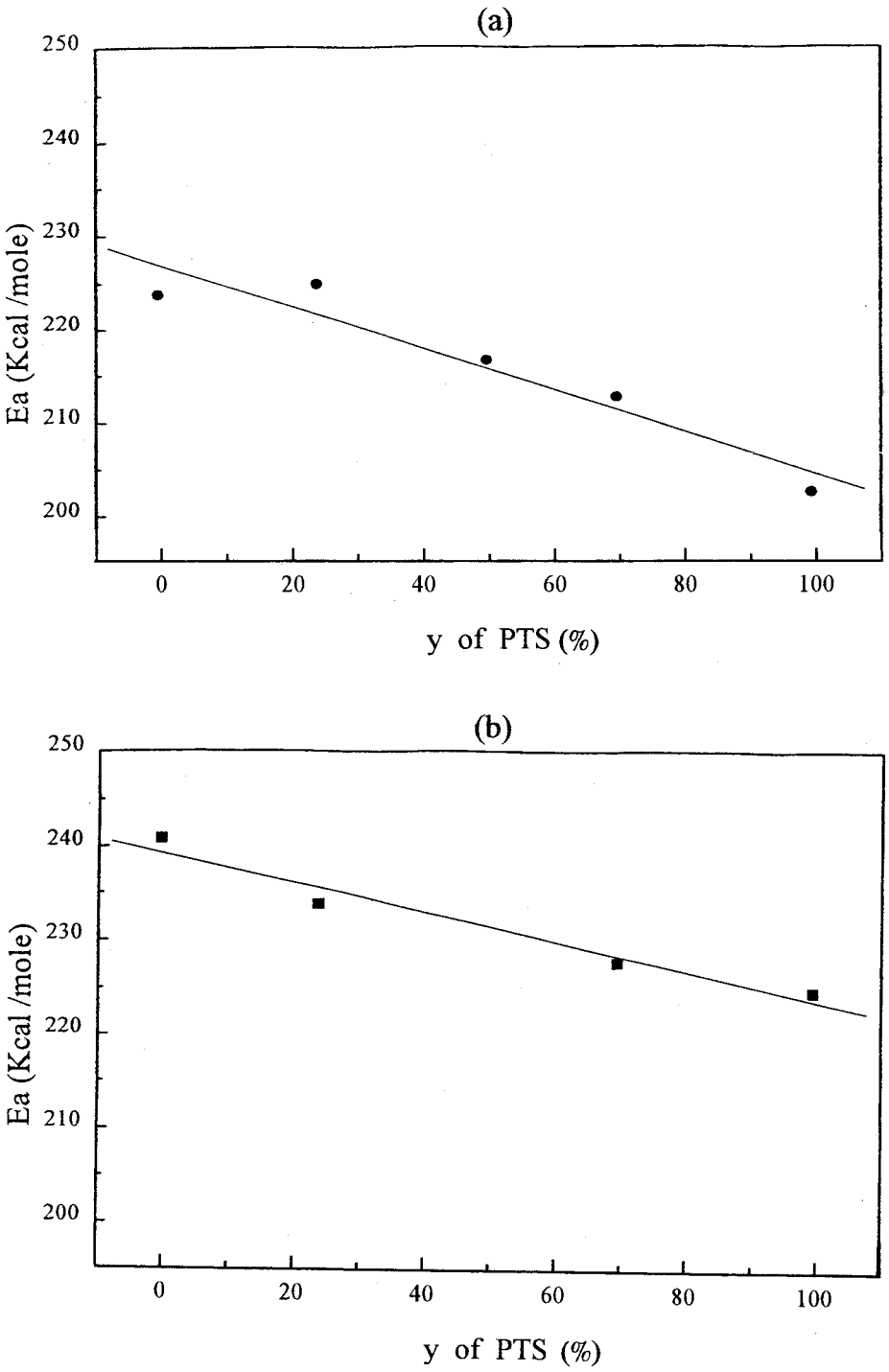

Figure 10 Activation energy of (a) 5000-PIS-*y*-PTS and (b) 10,000-PIS-*y*-PTS hybrid films.

shows the dependence of the densities of the hybrid films on the PTS content. Both 5000-PIS-*y*-PTS and 10,000-PIS-*y*-PTS films exhibited a similar trend: the higher the PTS content was, the lower the density of the films was. That means that bigger PSSQ-like domains decreased the density and enhanced the free volume of the *X*-PIS-*y*-PTS films. A higher PTS content could form bigger PSSQ-like domain sizes, leading to the introduction of more free volume and a lower dielectric constant. This has been discussed in another article.[12] Therefore, we conclude that adding

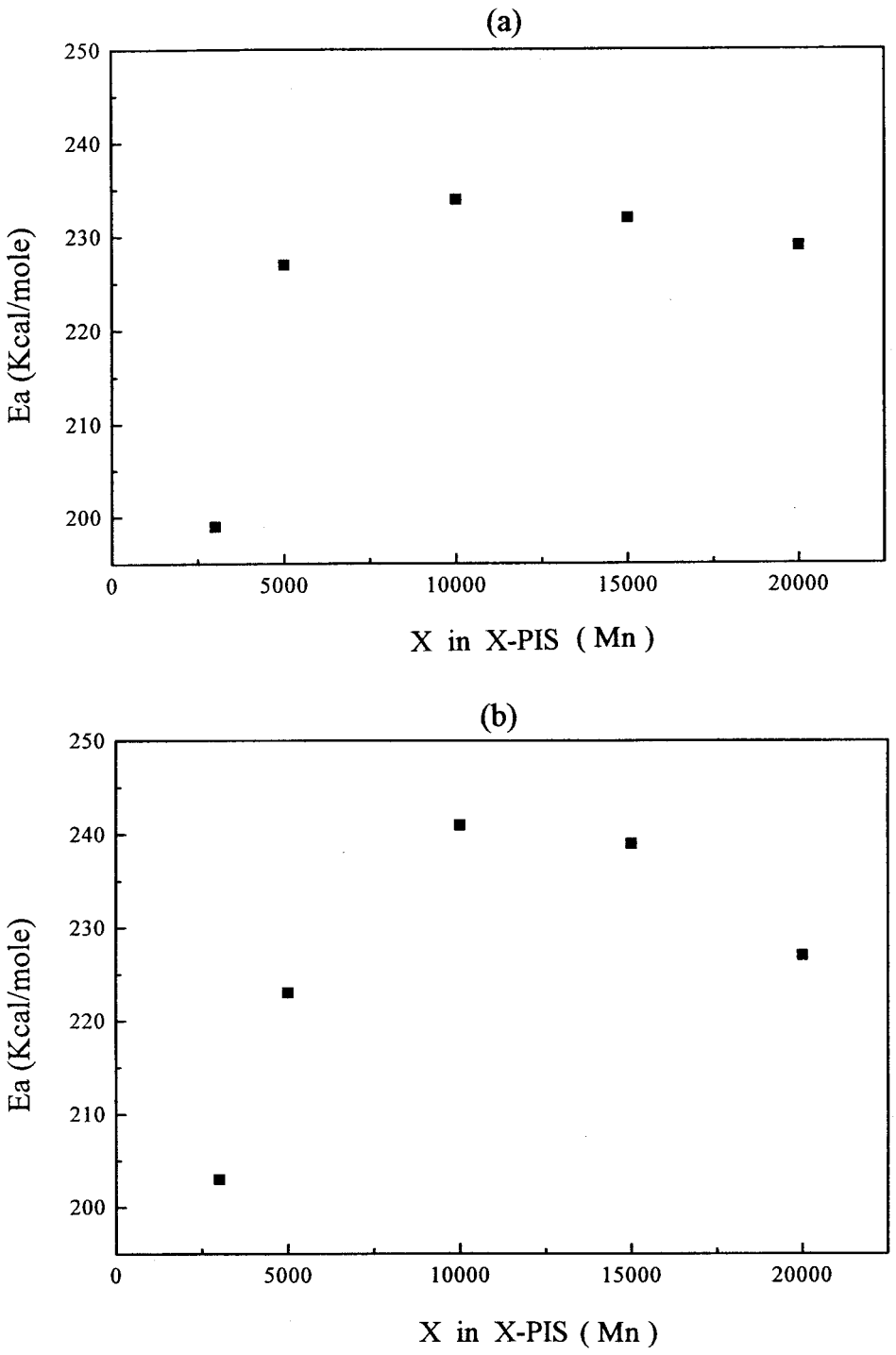

Figure 11 Activation energy of (a) *X*-PIS and (b) *X*-PIS-24-PTS hybrid films.

more PTS in *X*-PIS-*y*-PTS films enlarges the PI interblock parallel separation and decreases the interblock chain force. The weaker PI interblock chain force leads to a lower storage modulus and T_g. In the density-dependence curves at a lower PTS content, 10,000-PIS-*y*-PTS films had a higher density than the corresponding 5000-PIS-*y*-PTS films. However, at higher PTS contents, the former type of the hybrid film had lower densities than the corresponding latter types. 10,000-PIS-*y*-PTS films were more sensitive to the PTS content than 5000-PIS-*y*-PTS films.

As dynamic mechanical tests were subjected to different test frequencies, different T_g's could be observed. The activation energy of the α transition can be calculated from the following equation:[12–14]

$$\ln f_1/\ln f_2 = \Delta E a(1/T_2 - 1/T_1)/R$$

where ΔE_α is the activation energy, R is the gas constant, T_1 and T_2 are absolute temperatures (K), and f_1 and f_2 are test frequencies. Figure 7 shows experimental data (storage modulus and tan δ) for 10,000-PIS-100-PTS at five different frequencies (0.1, 0.5, 1, 5, and 10 Hz). The shift of the tan δ peak to higher temperatures with increasing frequency occurred in accordance with the time–temperature superposition. In this study, the damping peak temperature of the hybrid films increased 5–7°C as the frequency increased 1 order of magnitude. To obtain the Arrhenius activation energy of the α-relaxation process, one can plot a relationship between the logarithmic frequency and the reciprocal of the peak temperature for the α-relaxation process. Figures 8 and 9 show the linear relationship for the pure PI, *X*-PIS, *X*-PIS-24-PTS, 5000-PIS-*y*-PTS, and 10,000-PIS-*y*-PTS hybrid films with different slopes ($-E_\alpha/R$). The slope is proportional to the minus activation energy of its α-relaxation process. Activation energies of 5000-PIS-*y*-PTS hybrid films with different PTS contents are shown in Figure 10(a). With increasing PTS content, the activation energy decreased. As discussed, the free volume and the PI interblock separation increased with the PTS content. The greater separation and free volume made the movement of the PI chain easier and lowered the activation energy of the α-relaxation process. In 1000-PIS-*y*-PTS hybrid films, the dependence of the activation energy on the PTS content also showed the same trend. The activation energy in pure ODA–ODPA PI was the highest at 257 kcal/mol. This was probably caused by the least chain separation and free volume and the highest chain entanglement in the pure PI. Generally, the activation energy of glass-transition processes in polymers increases with the crosslinking density. However, in *X*-PIS films, the dependence of the activation energy on the PI block chain length exhibited a peak, not a linear relationship, as shown in Figure 11(a). The highest activation energy was located at a PI block molecular weight of 10,000 for both types of *X*-PIS and *X*-PIS-24-PTS films. This could have been caused by the two factors, crosslinking density and free volume, showing opposite effects in the α-relaxation process. In these two types of hybrid films, the increases in the PI block chain length led to a lower crosslinking density and a smaller free volume ratio. The lower crosslinking density promoted the chain motion, and the lower free volume hindered the chain motion. Therefore, the compromise of these two factors resulted in the highest value of the activation energy.

Table II Mechanical Properties of 5000-PIS Hybrid Films

	Properties		
X[b]-PIS	Tensile Strength (MPa)	Elongation at Break (%)	Tensile Modulus[a] (GPa)
3000-PIS	86.6 ± 9.6	2.9 ± 0.7	3.43 ± 0.18
5000-PIS	148.6 ± 4.1	11.0 ± 1.1	3.17 ± 0.09
10,000-PIS	138.4 ± 7.3	13.3 ± 1.5	2.60 ± 0.13
15,000-PIS	129.3 ± 5.0	14.6 ± 1.3	2.46 ± 0.08
20,000-PIS	116.6 ± 6.6	17.2 ± 2.1	2.01 ± 0.12
Pure PI	112.3 ± 3.2	29.6 ± 4.7	2.20 ± 0.08

The stress-strain tests were obtained from the average of five different determinations.

[a] Obtained from the initial slope of the stress–strain curves.

[b] The molecular weight of PI block chain length.

The mechanical properties of *X*-PIS hybrid films from stress–strain curves are shown in Table II. The tensile modulus decreased and the elongation increased with the PI block chain length. The tensile strength also exhibited a similar trend to that of the tensile modulus, except for an extraordinarily low tensile strength in the 3000-PIS film. This may have been caused by the rigidity of the hybrid film so that it broke at a relatively early stage during stressing. Table III shows the effect of the PTS content on the mechanical properties of the 5000-PIS-*y*-PTS hybrid films. A higher PTS content caused the tensile modulus and tensile strength to decrease but did not have a significant effect on elongation. This may show that the weak point of the hybrid films under stress was located in the PSSQ-like domains and that fracture started from the silica domain, although it constituted the three-dimensional network.

CONCLUSIONS

Pure aromatic ODA–ODPA PI is soluble in polar solvents, but its PI/PSSQ-like hybrid films are not

Table III Mechanical Properties of 5000-PIS-*y*-PTS Hybrid Films

	Properties		
y[b]	Tensile Strength (MPa)	Elongation at Break (%)	Tensile Modulus[a] (GPa)
0	148.6 ± 4.1	11.0 ± 1.1	3.17 ± 0.09
8	152.0 ± 3.8	13.6 ± 1.5	3.18 ± 0.05
24	142.8 ± 5.9	12.3 ± 0.7	2.95 ± 0.07
36	127.3 ± 8.1	13.8 ± 1.2	2.59 ± 0.10
50	119.9 ± 7.5	13.6 ± 0.4	2.43 ± 0.08
70	113.5 ± 6.5	14.1 ± 0.8	2.26 ± 0.09
100	89.1 ± 11.0	9.2 ± 2.7	1.96 ± 0.12

The stress–strain tests were obtained from the average of five different determinations.

[a] Obtained from the initial slope of the stress–strain curves.

[b] The weight ratios (%) of PTS to APTS–PAA.

soluble in organic solvents because the latter consists of linear PI blocks and a crosslinked PSSQ-like structure. The PI/PSSQ-like hybrid films have higher char yields than the pure PI film.

In *X*-PIS films, shortening the PI block chain length enhances the storage modulus and the tensile modulus. This is caused by the higher crosslinking density, leading to a stronger network structure and higher rigidity. The tan δ curves show two relaxation peaks, one at a low temperature of about 125°C, a β-transition, and the other at a higher temperature greater than 250°C, an α transition. The T_g's of *X*-PIS films decrease with the chain length, but the damping peak intensity increases with the chain length. The density of the *X*-PIS films increases with the PI block chain length. That means that in *X*-PIS films, the separation of the interblock PI chains and the free volume decrease with the PI block chain length and increase with the density. The dependence of activation energy on the PI chain length in *X*-PIS films shows a maximum at the PI chain length of 10,000. The appearance of the maximum value is caused by two conflicting structure factors affecting the α-relaxation process: the shorter the PI block chain length is, the higher the crosslinking density, the greater the interblock separation of the PI chains, and the lower the interblock chain interaction. In the stress–strain tests, the elongation increases with the PI block chain length.

In the series of *X*-PIS-*y*-PTS films, DMA data show that introducing PTS into the *X*-PIS structure to form greater PSSQ-like domains causes the storage modulus, T_g, damping peak intensity, and density to decrease. It seems that a more PSSQ-like structure in the hybrid films leads to more free volume or greater interblock separation. It, in truth, lowers the density, storage modulus, T_g, and damping peak. Therefore, the activation energy of the α-relaxation process in *X*-PIS-*y*-PTS films also decreases with the PTS content. The elongation at the break is independent of the PTS content in this type of film.

REFERENCES

1. Hedrick, J. L.; Cha, H. J.; Miller, R. D.; Yoon, D. Y.; Brown, H. R.; Srinivasan, S.; Di Pietro, R.; Cook, R. F.; Hummel, J. P.; Klaus, D. P.; Liniger, E. G.; Simonyi E. E. Macromolecules 1997, 30, 8512.
2. Chen, W. C.; Lin, S. C.; Dai, B. T.; Tsai, M. S. J Electrochem Soc 1999, 146, 3004.
3. Chen, W. C.; Yen, C. T. J Polym Res 1999, 6, 197.
4. Polyimides: Fundamentals and Applications; Ghosh, M. K.; Mittal, K. L., Eds.; Marcel Dekker: New York, 1996.
5. Polyimides: Synthesis, Characterization, and Applications; Mittal, K. L., Ed.; Plenum: New York, 1984.
6. Polyimides and Other High-Temperature Polymers; Abadie, J. M.; Sillion, B., Eds.; Elsevier: New York, 1991.
7. Jwo, S. L.; Whang, W. T.; Hsieh, T. E; Pan, F. E.; Liaw, W. C. J Polym Res 1999, 6, 175.
8. Okugawa, Y.; Yoshida, T.; Suzuki, T.; Nakayoshi, H. IEEE 1994, 570.
9. Kaltenecker-Commercon, J. M.; Ward, T. C.; Gungor, A.; McGrath, J. E. J Adhes 1994, 44, 85.
10. Cho, K.; Lee, D.; Ahn, T. O.; Seo, K. H.; Jeong, H. M. J Adhes Sci Technol 1998, 12, 253.
11. Lee, Y. D.; Lu, C. C.; Lee, H. R. J Appl Polym Sci 1990, 41, 877.
12. Tsai, M. H.; Whang, W. T. Polymer 2001, 42, 4197.
13. Hedrick, J. L.; Cha, H. J.; Miller, R. D.; Yoon, D. Y.; Brown, H. R.; Srinivasan, S.; Di Pietro, R.; Cook, R. F.; Hummel, J. P.; Klaus, D. P.; Liniger, E. G.; Simonyi E. E. Macromolecules 1997, 30, 8512.
14. Srinivasan, S. A.; Hedrick, L. J.; Miller, R. D.; Di Pietro, R. Polymer 1997, 38, 3129.
15. Iyoku, Y.; Kakimoto, M.; Imai, Y. High Perform Polym 1994, 6, 53.
16. Iyoku, Y.; Kakimoto, M.; Imai, Y. High Perform Polym 1994, 6, 43.
17. Mascia, L.; Kioul, A. Polymer 1995, 36, 3649.
18. Morikawa, A.; Iyoku, Y.; Kakimoto, M.; Imai, Y. Polym J 1992, 24, 107.
19. Tsai, M. H.; Whang, W. T. J Polym Res, to appear.

20. Mechanical Properties of Polymers and Composites; Nielsen, L. E., Ed.; Marcel Dekker: New York, 1974; Vol. 2.
21. An Introduction to the Mechanical Properties of Solid Polymer; Ward, I. M.; Hadley, D. W., Eds.; Wiley: New York, 1993.
22. Dynamic Mechanical Analysis of Polymeric Material; Murayama, T., Ed.; Elsevier: New York, 1978.
23. Mechanical Properties of Solid Polymers; Ward, I. M., Ed.; Wiley: New York, 1983.
24. Sysel, P.; Pulec, R.; Maryska, M. Polym J 1997, 7, 607.
25. Schrotter, J. C.; Smaihi, M.; Guizard, C. J Appl Polym Sci 1996, 61, 2137.
26. Smaihi, M.; Schrotter, J. C.; Lesimple, C.; Prevost, I.; Guizard, C. J Membr Sci 1999, 161, 157.
27. Mark, E.; Shen, D.; Wu, Z.; Lee, C. J.; Harri, F. W.; Cheng, Z. D. Polymer 1994, 34, 3209.
28. Sun, Z.; Dong, L.; Zhuang, Y.; Cao, L.; Ding, M.; Feng, Z. Polymer 1992, 33, 4728.
29. Huang, W.; Li, Y.; Xu, J.; Ding, M. Polymer 1997, 38, 4261.
30. Chern, Y. T.; Shiue, H. C. Macromolecules 1997, 30, 5766.